

# PCCP

Accepted Manuscript



This article can be cited before page numbers have been issued, to do this please use: L. Sonntag, F. Eichler, N. Weiß, L. Bormann, D. S. Ghosh, J. M. Sonntag, R. Jordan, N. Gaponik, K. Leo and A. Eychmueller, *Phys. Chem. Chem. Phys.*, 2019, DOI: 10.1039/C9CP00680J.



This is an Accepted Manuscript, which has been through the Royal Society of Chemistry peer review process and has been accepted for publication.

Accepted Manuscripts are published online shortly after acceptance, before technical editing, formatting and proof reading. Using this free service, authors can make their results available to the community, in citable form, before we publish the edited article. We will replace this Accepted Manuscript with the edited and formatted Advance Article as soon as it is available.

You can find more information about Accepted Manuscripts in the [author guidelines](#).

Please note that technical editing may introduce minor changes to the text and/or graphics, which may alter content. The journal's standard [Terms & Conditions](#) and the ethical guidelines, outlined in our [author and reviewer resource centre](#), still apply. In no event shall the Royal Society of Chemistry be held responsible for any errors or omissions in this Accepted Manuscript or any consequences arising from the use of any information it contains.

## ARTICLE

## Influence of the average molar mass of poly(N-vinylpyrrolidone) on dimensions and conductivity of silver nanowires

Luisa Sonntag,<sup>a,d</sup> Franziska Eichler,<sup>a</sup> Nelli Weiß,<sup>a</sup> Ludwig Bormann,<sup>b</sup> Dhriti S. Ghosh,<sup>b</sup> Jannick M. Sonntag,<sup>c</sup> Rainer Jordan,<sup>c,d</sup> Nikolai Gaponik,<sup>\*a,d</sup> Karl Leo,<sup>b,d</sup> and Alexander Eychmüller<sup>a,d</sup>

Received 00th January 20xx,  
Accepted 00th January 20xx

DOI: 10.1039/x0xx00000x

We investigate the influence of the average molar mass ( $M_w$ ) of the capping agent poly(N-vinylpyrrolidone) (PVP) on the conductivity of a silver nanowire (AgNW) network. Within the polyol process, the chain length of PVP is known of influencing the AgNW diameters and lengths. By altering the reaction temperature and time and using PVP of different chain lengths, we synthesized AgNWs with varying diameter, length and PVP coverage. The obtained plethora of AgNWs is the basis for conductivity investigations of networks fabricated of AgNWs with a diameter of either 60 nm or 80 nm. The results show a negative influence of long-chain PVP on the conductivity of the subsequent network if 60 nm thick AgNWs are utilized. Overall, we obtain well performing AgNW transparent electrodes on glass with  $R_s = 24.4 \Omega/\text{sq}$  at 85.5 % $T_{550\text{nm}}$ .

### Introduction

Transparent conductive electrodes (TCE) fabricated of silver nanowire (AgNW) networks are highly promising candidates for the implementation in optoelectronic devices, such as solar cells, light-emitting-diodes, or touch screens.<sup>1–6</sup> AgNW electrodes show comparable sheet resistances ( $R_s$ ) and transmittances at 550nm (% $T_{550}$ ) as commercially used indium tin oxide (ITO). Since ITO is a ceramic, its brittleness may cause electrode failure after bending or stretching. Also, the ITO vapour deposition process is more expensive than wet-chemical film fabrication. Electrodes consisting of AgNWs on the other hand fulfil the requirements for high conductivity and transparency, while solution-based processing allows low cost and large area deposition techniques.<sup>7,8</sup> Furthermore, the ductility of silver enables the bend- and stretchability of AgNW networks on flexible substrates.<sup>9</sup>

Most synthetic approaches rely on the work of Wiley *et al.*, who introduced a one-pot polyol process for producing AgNWs.<sup>10</sup> Here, ethylene glycol (EG) is the solvent and subsequent

reducing agent and silver nitrate is the silver source. The key condition allowing an elongated growth into nanowires is the use of poly(N-vinylpyrrolidone) (PVP) as a capping agent, which is interacting with the {100}-facet of the silver nanowires leading to a preferential deposition of new silver atoms at the {111}-facet.<sup>11</sup> Our work is based on an improved one-pot polyol process proposed by Bergin *et al.*, where the addition of  $\text{Fe}(\text{NO})_3$  and NaCl reduces oxygen etching and provides a high yield on multi twinned particles (MTPs), which finally grow into the desired AgNWs.<sup>12</sup> Earlier research has shown that the reaction temperature, as well as the reaction time have a major influence on the AgNW diameter  $D$  and length  $L$ . Here, a higher reaction temperature leads to an increased seed formation resulting in thinner and usually shorter AgNWs.<sup>12</sup>

In the past, several groups investigated the influence of the mass average molar mass ( $M_w$ ) of PVP on the AgNW synthesis. Their findings regarding the role of PVP are diverse and based on different synthetic methods. The most agreed requirement to successfully synthesize AgNWs is using PVP with a critical minimum molar mass. These were 10 kDa,<sup>13</sup> 40 kDa,<sup>14</sup> ~50 kDa,<sup>15–18</sup> or even 1,300 kDa.<sup>19</sup> Utilizing PVP of a lower  $M_w$  leads to nanorods and nanoparticles of undefined shapes as main or byproduct and no AgNWs or only in a low yield. Some groups also observed an increase of the nanowire aspect ratio (*aspect ratio*  $A = \text{length}/\text{diameter}$ ) with increasing  $M_w$  of PVP.<sup>13–15</sup> Regarding the diameter controversial outcomes were stated: an increase,<sup>18</sup> a decrease,<sup>15</sup> or no change of diameter<sup>16</sup> with increasing  $M_w$  of PVP. A mixture of PVP with two different  $M_w$  resulted in thinner AgNWs with high aspect ratios.<sup>17,20</sup> Details of the synthetic approaches and the results regarding the influence of PVP reported in the literature up to date are summarized in Table 1.

<sup>a</sup> Physical Chemistry, Technische Universität Dresden, Bergstraße 66b, 01062 Dresden, Germany.

<sup>b</sup> Dresden Integrated Center for Applied Physics and Photonic Materials (IAPP), Technische Universität Dresden, Nöthnitzer Str. 61, 01187 Dresden, Germany.

<sup>c</sup> Chair of Macromolecular Chemistry, Faculty of Chemistry and Food Chemistry, School of Science, Technische Universität Dresden, Mommsenstr. 4, 01069 Dresden, Germany.

<sup>d</sup> Center for Advancing Electronics Dresden (cfaed), Technische Universität Dresden, 01062 Dresden, Germany.

nikolai.gaponik@chemie.tu-dresden.de

alexander.eychmueller@chemie.tu-dresden.de

Electronic Supplementary Information (ESI) available: [details of any supplementary information available should be included here]. See DOI: 10.1039/x0xx00000x



Unfortunately, PVP has the drawback of forming an insulating layer around the NW. This hinders tight AgNW contacts and decreases the conductivity of the AgNW network. To improve the AgNW electrode performance, post treatments like heating,<sup>21</sup> low-temperature annealing,<sup>22,23</sup> mechanical pressing,<sup>24,25</sup> or chemical welding<sup>26,27</sup> are necessary.

To the best of our knowledge, investigations of the influence of the average molar mass of PVP on the conductivity of a post-treated AgNW electrode do not exist in the literature. Therefore, next to examining the PVP influence on the AgNW dimensions, we focus on investigating if the variation of  $M_w$  of PVP has an impact on the conductivity of the transparent AgNW network after annealing.

Taking into account that the dimensions of the AgNWs correlate strongly with the resulting network conductivity,<sup>12</sup> the experiment can therefore only be accomplished with AgNWs of the same dimensions, but different PVP shells regarding their  $M_w$ . Attempting to maintain the same dimensions of the AgNW network synthesized with various PVPs, an extensive variation of reaction temperature and reaction time was performed in the frame of the present work.

Transparent electrodes were fabricated utilizing a large-scale spray coating process, followed by annealing and their conductivities were compared. Finally, the best performing electrode was incorporated in a small molecule organic solar cell to demonstrate its compatibility with typical processing technologies used in organic electronics.

## Results and discussion

View Article Online

DOI: 10.1039/C9CP00680J

First, we synthesized AgNWs with comparable dimensions, but different PVP shell in order to further determine the influence of the average molar mass of PVP on the conductivity of the AgNW network. A detailed overview of the obtained AgNW diameters and lengths is given in Figure 1. The results are ordered according to the used  $M_w$  of PVP in the respective segments by the reaction temperature and the corresponding reaction time. The colours represent the same reaction temperature and time. We utilized PVP with either  $M_w = 10$  kDa, 40 kDa, 55 kDa, 360 kDa or 1,300 kDa, referred to as PVP10, PVP40, PVP55, PVP360 and PVP1300, respectively.

### Temperature dependence within AgNW synthesis

In our experiments the polyol process was carried out varying the temperature between 135-150 °C and the reaction time between 5 and 2 h. To begin with, we compare the AgNW dimensions for performing the synthesis at 135°C for 5 h (blue) or 140 °C for 4 h (orange). Concerning the PVP types, the diameter is approximately the same, except for PVP55, where it is larger with 73 nm at 140°C than with 59 nm at 135°C. The AgNWs are much longer when the reaction is performed at the higher temperature. The exception here is PVP40, where the average length remained the same.

Table 1: Overview of investigations regarding the influence of the average molar mass of PVP on the synthesis and dimensions of AgNWs.

Synthetic approach, additives	PVP:Ag	PVP [kDa]	NW		Conclusion regarding PVP	Ref.
			D [nm]	L [μm]		
Microwave assisted., 198°C, 3-8 min, H <sub>2</sub> PtCl <sub>6</sub> ·6H <sub>2</sub> (seeds)	5.6 : 1	10, 40, 360	-	1-20	‡, length↑ and aspect ratio↑ with $M_w$ of PVP↑	13
Dropwise simultaneously 150 °C, 80 min	1 : 1	15, 38, 58, 200, 800	100-180	3-10	‡, yield↑, aspect ratio↑, diameter↓ with $M_w$ of PVP↑	15
One-Pot; FeCl <sub>3</sub> (dropwise) 130 °C, 5 h	1.2 : 1	6,10, 30, 40, 65,1300	-	-	‡, yield↑, aspect ratio↑ with $M_w$ of PVP ↑	14
One-Pot, FeCl <sub>3</sub> 140°C, 50 min	1.4 : 1	55, 360, 1300	25-160	5-50	Mixture of PVP55 and PVP360 (1:2) results in thin wires	20
One-Pot, NaCl 185°C, 20 min	3:1 (was varied)	8, 29, 40, 1300	90-300	1-6	‡, adsorption and steric effect of PVP discussed	19
One-Pot; NaCl, NaBr 170°C, 1 min	1.9 : 1	55, 130	20	40	‡, no influence of $M_w$ of PVP on diameter	16
Hydrothermal; 160°C, 3 h CuCl <sub>2</sub> ·2H <sub>2</sub> O (dropwise)	1.5 : 1 (was varied)	10, 40, 58, 360	47-235	6-70	‡, mixture of PVP results in thin wires	17
One-Pot; 160 °C, 1 h dropwise simultaneously	3 : 1 (was varied)	10, 55, 360	102-135	20-25	‡, diameter↑, length↓ with $M_w$ of PVP↑	18
One-Pot; Fe(NO <sub>3</sub> ) <sub>3</sub> , NaCl 140 °C, 2 h	1.5 : 1	10, 40, 55, 360,1300	33-262	1-42	‡, length↑, aspect ratio↑ with $M_w$ of PVP↑	Current work

‡: state critical minimum  $M_w$  of PVP; All approaches are using ethylene glycol, PVP and Ag(NO<sub>3</sub>)<sub>3</sub>, AgNW dimensions are given in diameter ( $D$ ) and length ( $L$ ) and the ratio of PVP:Ag is given in terms of monomeric units, respectively.



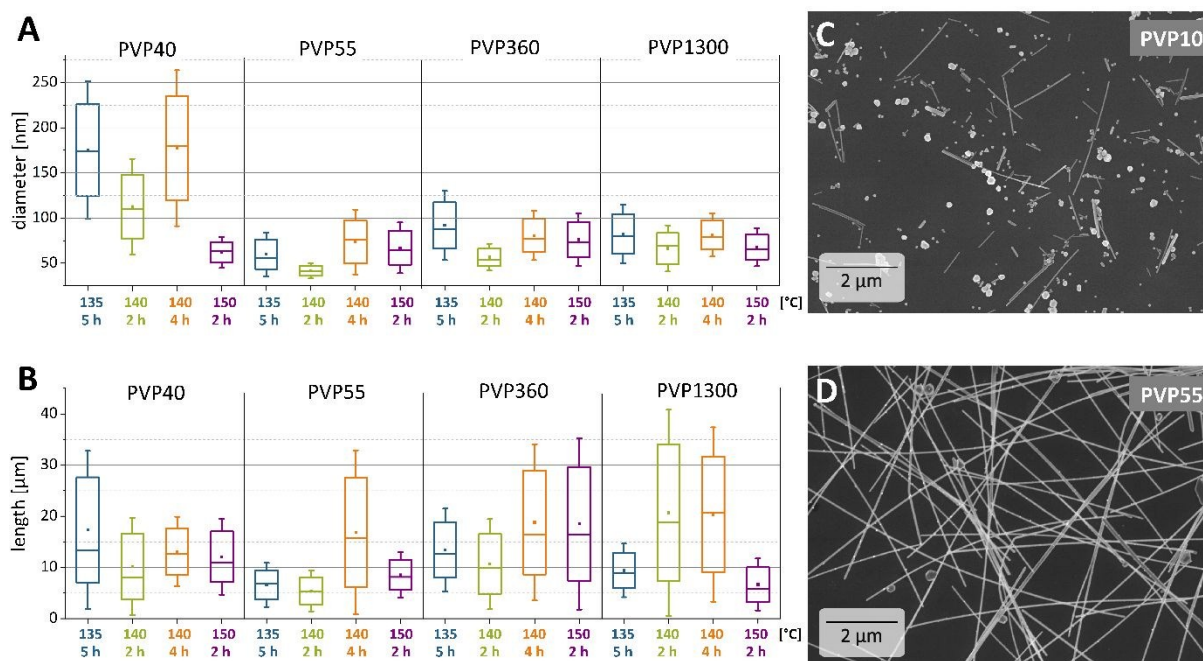


Figure 1: A) Diameters and B) lengths of AgNWs synthesized at different reaction temperatures, times and  $M_w$  of PVP. Corresponding colours in different frames reflect the same reaction temperature and time. C) SEM images of AgNWs synthesized at 140 °C for 2 h with C) PVP10 or D) PVP55.

In order to obtain even thinner wires, we stopped the reaction at 140 °C after 2 h (green) and in all cases the diameter and the length decreased with a shorter reaction time. The length decrease was not as pronounced when PVP1300 was used. We also carried out the synthesis at 150 °C for 2 h (purple). In comparison to 140 °C for the same time, we observed a slight decrease of the diameter except for the synthesis with PVP40. Therein the average diameter decreased significantly from 112 nm to 61 nm. There is no pronounced trend between the AgNW lengths when comparing these reaction temperatures. Bergin *et al.* reported about the temperature effect on the AgNW diameter and length. They stated that a higher reaction temperature leads to an increased seed formation resulting in thinner and usually shorter NWs.<sup>12</sup> They have also observed an increase of the diameter and length at a higher temperature, but same reaction time and explain this with a faster reduction rate of EG at higher reaction temperatures. Their findings are in accordance with our results with the exception that in our experiments the longest AgNWs grew at elevated temperatures (140 °C and 150 °C) instead of lower reaction temperatures. Possible reasons can be found in the slight deviation of the reaction procedure, *i.e.* in the treatment of heated EG with a  $N_2$  flow in our case as was also described in an earlier work by Wiley *et al.*<sup>28</sup> Furthermore, the higher temperatures could accelerate the growth rate and led to longer AgNWs.

#### $M_w$ of PVP dependence within AgNW synthesis

Next, the influence of the  $M_w$  of PVP is investigated. We, likewise previous works, found the need of a minimum PVP chain length to successfully obtain AgNWs. In our procedure,

the usage of PVP10 lead to nanoparticles, nanorods and only a minor amount of nanowires (Figure 1 C). Even though AgNWs were produced with the capping of PVP40, the as synthesized AgNWs show a broad distribution of both, diameter and length. Therefore the minimum  $M_w$  to synthesize AgNWs with a narrow diameter distribution was, in our case, 55 kDa (Figure 1 D). For the reactions carried out at 135 °C for 5 h (blue) and 140 °C for 2 h (green) or 4 h (orange), we could observe the same trend: the diameters of the NWs dropped from PVP40 to PVP55 and increased in case of PVP360 or PVP1300. The diameter difference if PVP360 or PVP1300 were used was however marginal. Moreover, at the higher reaction temperature of 150 °C (purple) the diameter difference between NWs synthesized with various  $M_w$  of PVP was only in a range of 2-11 nm. With respect to the aspect ratio, we observed by trend an increase of the aspect ratio if long chain PVP was utilized (Figure 1 A). The exception here is the synthesis at 150 °C for 2 h with PVP1300. Compared to PVP40 and PVP55, the presence of PVP360 or PVP 1300 caused an increase in the aspect ratio. Most pronounced at the reaction temperature of 140 °C for 2 h, the aspect ratio increased from 100 (PVP40) to 300 (PVP1300) (Figure 1 B). All together, we observed no distinct and unambiguous trends regarding the influence of  $M_w$  of PVP on either the diameter or the aspect ratio across all reaction conditions. However, some tendencies can be extracted from the comparative analysis of our data and the literature reports, as will be discussed in the following. According to simulations by Kyrychenko *et al.* reporting about the interactions between PVP of different chain lengths with Ag nanocrystals (NC), long-chain PVPs show a higher number of PVP-to-Ag contacts and a higher degree of



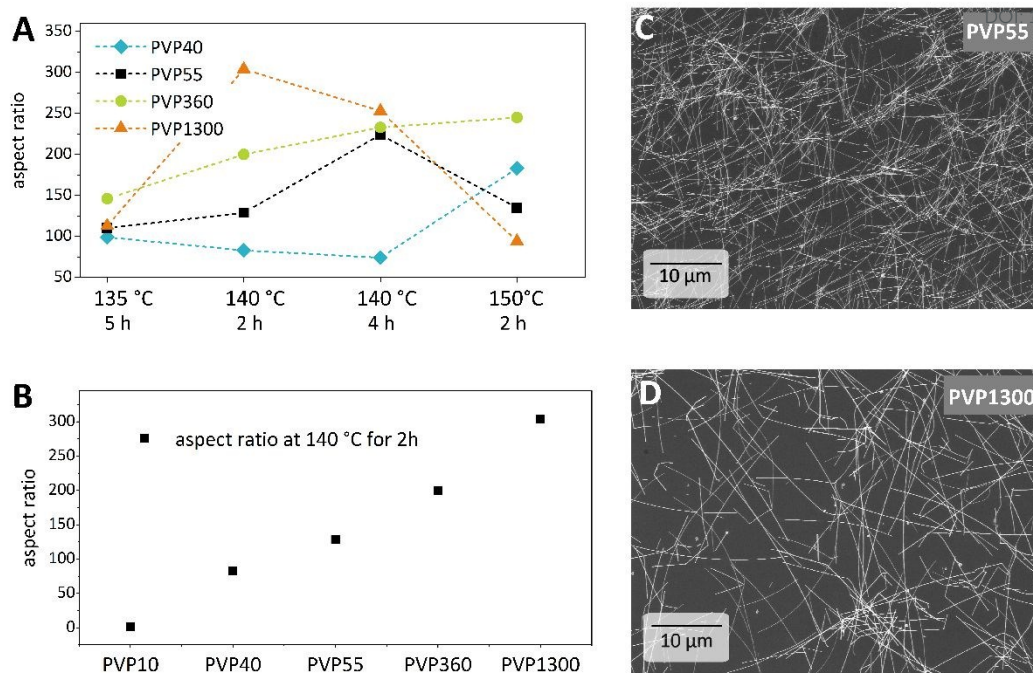


Figure 2: Aspect ratios of synthesized AgNWs with various  $M_w$  of PVP obtained at A) different reaction temperatures and times and B) 140 °C for 2h. SEM images of AgNWs synthesized at 140 °C for 2h in the presence of C) PVP55 or D) PVP1300.

polymer layers around the NC. These investigation would led to an assumption that the diameters of the nanowires would decrease with increasing chain-length of PVP in consequence of steric hindrance.<sup>29</sup> However, we observed a diameter decrease only when switching from PVP40 to PVP55. Utilizing PVP with longer chains (PVP360, PVP1300) an opposite behavior occurs. explain this, we propose that the PVP chain length is decisive not only for the governing of the AgNW growth, but already during the nucleation of the Ag nanoparticles. Since the quantity of pyrrolidone moieties remained constant, meaning that less numbers of polymer chains are present within the synthesis in respect of long-chain PVP, fewer Ag nuclei (five-fold twinned decahedra) can be stabilized during the nucleation. This leaves more precursor per nuclei in the reaction mixture. Additionally, the higher viscosity of PVP360 and PVP1300 solutions in EG may reduce the nucleation rate. Our further understanding is that Ag atoms are preferentially added to an existing AgNW if they are in close spatial proximity. This is also probably the case for a coordinated  $Ag^+$  at a carbonyl group within the same polymer chain which is attached to the side of a growing AgNW in comparison to a  $Ag^+$  at an adjacent carbonyl group elsewhere in the solution. Consequently, the longer the PVP chain, the more  $Ag^+$  are present along the polymer chain to be added to an existing AgNW leading to a diameter growth because of a higher degree of shelling. The combination of these effects could result in AgNW with enlarged diameters. The increase of the aspect ratio with  $M_w$  of PVP can be explained by the following: a longer polymer chain promotes the growth of high aspect AgNWs due to a greater number of contacts between Ag and long-chain PVP, as well as a higher degree of layering around the AgNW as mentioned before.<sup>29</sup> PVP1300

promoted the growth of AgNWs with up to 60  $\mu m$  in length and PVP55 the growth of a maximum of 10  $\mu m$  long NWs (Figure 2 C, D). This could be due to the fact that a longer PVP chain leads to a better stabilization due to a high number of contacts between PVP and Ag. Furthermore, as aforementioned, the high number of  $Ag^+$  coordinated at the longer polymer chain can readily attach at the ends of the existing AgNW rather than adding on to an adjacent one.

Altogether, the trends how the  $M_w$  of PVP affects the AgNW dimensions reported in the literature are sometimes contradictory. We suspected that the polydispersity of the commercially available PVP batches could be responsible for this. Indeed, size exclusion chromatography (SEC) revealed broad dispersities ( $D = M_w/M_n$ ) higher than 3, meaning the PVP powders are mixtures of strongly differing chain lengths (Figure S. 1). This high polydispersity can explain the discrepancies of the influence of  $M_w$  of PVP on the AgNW dimensions reported in both, our work and in the above mentioned literature. Therefore, investigations of the used PVP is recommended and utilization of controlled polymerized PVP owing narrow dispersities may give specified results. In general, there remains a lack of full understanding about the conformation, coil size, fluctuation, viscosity and influence of the polymer chain during the synthesis of AgNWs.

#### Role of PVP in the electrode performance

Despite repeated washing, it is generally known that a PVP layer remains around the AgNW. High resolution transmission microscopy (HR-TEM) revealed 1-4 nm thick shells around the



Table 2: Dimensions overview of AgNWs differing in PVP shell used for heat treatment. The dimensions are given in diameter ( $D$ ), length ( $L$ ) and aspect ratio ( $A$ ). [View Article Online](#)  
DOI: 10.1039/C9CP00680J

	AgNW60-PVP40	AgNW60-PVP55	AgNW60-PVP360	AgNW60-PVP1300	AgNW80-PVP55	AgNW80-PVP360	AgNW80-PVP1300
$D$ [nm]	61 ± 12	64 ± 4	56 ± 10	66 ± 17	73 ± 24	81 ± 18	82 ± 21
$L$ [μm]	12.0 ± 8,3	9.3 ± 6.8	10.6 ± 6.3	20 ± 14.2	16.9 ± 10.7	18.8 ± 10.1	9.4 ± 3.5
$A$	196	145	189	303	232	232	114

AgNWs independent of  $M_w$  of PVP. Figure 3 A exemplarily shows a AgNW with an amorphous PVP coating. With higher magnification, the crystal properties can be evaluated showing a lattice distance of 2.35 Å at the elongated side of the AgNW corresponding to the {100}-facet (Figure 3 B). However, the PVP shell is not clearly recognizable anymore.

As described above with variation of synthetic parameters such as temperature, reaction time and molar mass of PVP we produced AgNWs with average diameters from 41 to 137 nm and lengths from 3 to 20 μm. Since a comparison of the electrical performance is only possible with AgNWs of the same dimensions,<sup>12</sup> we chose AgNWs with nearly equal lengths from this plethora of synthesized AgNWs for the investigation of the influence of  $M_w$  of PVP on the conductivity of annealed AgNW networks. Herein, AgNWs with 60 nm and 80 nm diameters covered with either PVP40, PVP55, PVP360 or PVP1300 were chosen as representative examples. Their diameter, length and corresponding aspect ratio are summarized in Table 2. Detailed information can be found in Figure S. 2. To distinguish the optimum annealing temperature, AgNWs were spray-coated onto glass substrates to reach a similar transmission at 550 nm ( $\%T_{550nm}$ ) of approximately 83% and the electrodes were then gradually heated from 75 °C to 250 °C on a hot plate for 20 min at each temperature. Between the heating steps the sheet resistance ( $R_s$ ) was measured ( $R_s$  vs.  $T$  are shown in Figure S. 3). For all electrodes there are two stages distinguishable. First, the electrical resistance dropped until a minimum  $R_s$  was reached with a heat treatment of 200 °C. After heating the electrodes to 225 °C, the conductivity diminished. The annealing steps can be evaluated as follows: in the beginning, the PVP on the AgNW surface are partially desorbed, which improves the contact of adjacent AgNWs and  $R_s$  decreased. At the glass temperature of PVP, i.e. 140-180 °C,<sup>30-33</sup> the PVP shell softens and flows, further improving the junction contact. After an additional temperature increase, a partial degradation of PVP as well as local sintering at AgNW junctions due to diffusion enhances the electrical

performance.<sup>34</sup> Further temperature elevation (225-250 °C) lead to coalescence of the unprotected AgNWs into disconnected droplets due to the Plateau-Rayleigh instability (Figure 3 C).<sup>35</sup> The latter is the decay of a cylindrical body into a particle chain driven by the instability caused by capillary force. The driving force is the minimization of the surface energy. Hereby, the mass transport occurs *via* surface diffusion and the volume is conserved during fragmentation. This behaviour has been studied on thermally treated AgNWs,<sup>35</sup> copper nanowires,<sup>36</sup> and laser induced spheroidisation of metal films.<sup>37</sup> Also, Monte-Carlo simulations of thermal annealing of germanium nanowires predicted comparable fragmentations.<sup>38</sup> To receive an insight of the variances between the above mentioned electrodes, we measured the  $R_s$  at different %T. Hereby, after spray-coating only one annealing step was applied at the optimum annealing temperature of 200 °C for 20 min. The data was fitted using a model proposed by De *et al.*<sup>39</sup> to distinguish the performance in the percolative and bulk regime (Figure 4 A, B). High transmittance electrodes qualifying for optoelectronic device implementation are assigned to the percolative regime (80-99%). In the following the electrical performances of the AgNW60 and AgNW80 electrodes are compared at the same transmission of 84% $T_{550nm}$ . We found AgNW60 electrodes performing best if covered with shorter chain PVP as sheet resistances are 18 Ω/sq (PVP40) and 17 Ω/sq (PVP55), respectively. The resistances were higher if AgNW60 were covered with PVP360 (26 Ω/sq) or PVP1300 (22 Ω/sq). Regarding the AgNW80, two systems perform equally well despite different PVP coating:  $R_s = 25$  Ω/sq (PVP55) and  $R_s = 28$  Ω/sq (PVP360). Here, AgNW80 with PVP1300 had the worst electrical performance with 90 Ω/sq. We have to note, that not only the PVP coverage can be taken into account to evaluate the performance of the electrodes. According to Bergin *et al.* the electrode transmittance increases with nanowire length at a given sheet resistance which is due to the fact that less nanowire connections are necessary to achieve percolation.<sup>12</sup>

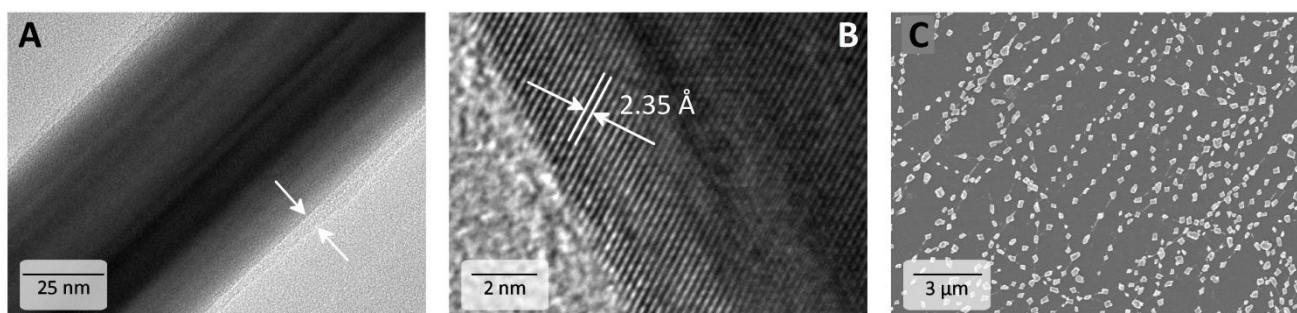


Figure 3: A) TEM image of a AgNW clearly shows a PVP shell, B) HR-TEM Image of a AgNW showing a lattice distance of 2.35 Å corresponding to the {100}-facet, C) SEM image of a destroyed AgNW network after gradual annealing until 250 °C.



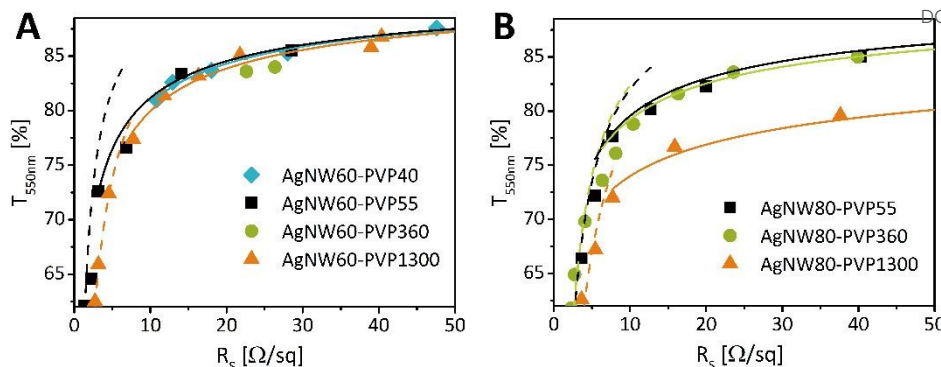


Figure 4: Sheet resistance versus transmittance at 550 nm of AgNWs varying in PVP-shell with A) 60 nm and B) 80 nm. Dashed lines correspond to bulk behavior, continuous line correspond to percolative behavior. Fitted with a model presented by De *et al.*<sup>39</sup>

Solely looking at the AgNW morphologies, a higher aspect ratio is expected to show better conductivity.<sup>17</sup> Even though AgNW60-PVP1300 ( $A = 303$ ) and AgNW60-PVP360 possess the higher aspect ratios, it is outperformed by both, AgNW60-PVP40 ( $A = 196$ ) and AgNW60-PVP55 ( $A = 145$ ), respectively. Regarding the performance of AgNW80, the influence of the  $M_w$  is not as strong as the impact of the aspect ratios of AgNW80-PVP55 and AgNW80-PVP360, which are the same ( $A = 232$ ) and whose  $R_s$  differ slightly.

The lower electrical performance of AgNW80-PVP1300 can be explained by the more pronounced impact of the small aspect ratio of 114. The results show an inhibitory effect of long-chain PVP on the network conductivity for AgNW60 in spite of annealing. We suggest that the relatively lower influence of  $M_w$  of PVP for AgNW80 can be attributed to a higher ratio of the AgNW diameter to the thickness of the PVP layer. We understand that for thicker NWs a contribution of the NW diameter to the final conductivity dominates over the influence of the PVP layer.

Concluding these investigations, the AgNW morphology and aspect ratio play a fundamental role in the overall performance of conductive networks. While the network conductivity prepared with AgNW80 is not as strongly affected by  $M_w$ , there is a negative impact of higher  $M_w$  on networks consisting of AgNW60. Therefore, preferentially shorter chain PVP should be favored for the synthesis of thin AgNWs with regards to well conducting networks. Utilizing thin or ultra-thin AgNWs is mainly desired for the implementation into devices if low-haze electrodes are required, for instance into LEDs.<sup>8</sup> Particularly, thin-film organic optoelectronic devices suffer from short circuits if AgNWs reach into the upper layers.<sup>40</sup> The surface roughness of thin NWs is not as pronounced as compared to thicker ones, which reduces the necessary amount of surface flatteners.<sup>41</sup>

### Solar cell integration

To demonstrate the applicability of the investigated materials, the electrode AgNW60-PVP40 was integrated in an organic solar cell (OSC). Details such as a schematic layer stack, current density versus voltage ( $jV$ ) characteristics and a summary of the

electrode and photovoltaic performance can be found in the supporting information (Table S 1, Figure S. 4). The AgNW electrode on glass is characterized by 85.5% transmittance at 550 nm and a sheet resistance of 24.4  $\Omega/sq$ . In comparison, the ITO electrode shows  $R_s = 30.4 \Omega/sq$  at 80.8% $T_{550nm}$ . The inherently rough AgNW network needs to be smoothed with an additional planarization layer. For this purpose, PEDOT:PSS is spin-coated directly on the structured AgNW electrode. Briefly, the small molecule material DCV5T-Me and  $C_{60}$  are used as donor and acceptor molecules in a bulk heterojunction with n-i-p architecture, respectively.<sup>42</sup> We show working OSCs with an efficiency of 2.4% on in-house synthesized and fabricated AgNW/PEDOT:PSS electrodes, being comparable to a ITO/PEDOT:PSS reference devices with 3.4%. In comparison to pristine ITO (PCE of 7.1%), the addition of PEDOT:PSS caused an efficiency decrease. The utilized OSC layer stack is optimized for ITO and the AgNW based device performance could further be improved by adjusting the organic layers to the AgNW/PEDOT:PSS film thickness. Also, AgNW electrodes exhibit a low specular reflection  $R_{vis}$  which does not support a microcavity effect.<sup>43</sup>

### Conclusions

We investigated the role of the average molar mass of PVP ( $M_w$ ) within the polyol process in order to obtain AgNWs. By varying the reaction temperature and time as well as using PVP of different mass average molar mass, a variety of different AgNWs could be synthesized which differ in diameter and length. Subsequently, AgNW electrodes were fabricated with AgNWs of similar dimension but varying PVP shell. The AgNW dimensions control the main part on the network conductivity. Despite heat treatment we observed an inhibitory effect of the longer chain PVP for AgNWs with 60 nm. This inhibition was not as pronounced for AgNWs with 80 nm. Utilizing size exclusion chromatography, we determined that commercially available PVP batches were broadly distributed regarding the average molar mass. This can explain the diversity of the research results concerning the influence of  $M_w$  of PVP on AgNW dimensions. The fabricated transparent electrodes showed a reasonably low sheet resistance of  $R_s = 24.4 \Omega/sq$  at 85.5% $T_{550nm}$  and can be



incorporated in combination with PEDOT:PSS into a DCV5T-Me:C60 organic solar cell.

## Experimental

### Materials

The following chemicals and solvents were used to synthesize AgNWs. Silver nitrate ( $\text{AgNO}_3$ ,  $\geq 99.9\%$ ), poly(N-vinylpyrrolidone) (PVP,  $M_w \approx 10,000$  g/mol ( $\bar{D} = 3.5$ ), 40,000 g/mol (K30,  $\bar{D} = 3.9$ ), 55,000 g/mol ( $\bar{D} = 5.2$ ), 360,000 g/mol ( $\bar{D} = 4.8$ )) were purchased from Sigma Aldrich, PVP with  $M_w \approx 1,300,000$  g/mol ( $\bar{D} = \text{N/A}$ ) from Alfa Aesar, iron (III) nitrate nonahydrate ( $\text{Fe}(\text{NO}_3)_3 \cdot 9\text{H}_2\text{O}$ ,  $\geq 90\%$ ) from Merck, PEDOT:PSS 'P VP Al 4083' (Al4083) from Heraeus Clevios, Germany, ethylene glycol ( $\geq 99.0\%$ ) from J.T. Baker, sodium chloride (NaCl, 100 %) and ethanol (absolute) from AnalaR NORMAPUR, acetone (p.A.) from Fischer. Milli-Q<sup>®</sup>-water (Millipore) water was used.

### Synthesis of silver nanowires

The synthesis of AgNWs was carried out based on a polyol approach reported by Bergin et al.<sup>12</sup> First, 39.6 ml ethylene glycol (EG) was added in a 100 ml flask and heated up to the desired temperature in an oil bath. The EG was kept at the set temperature for 1 h under constant agitation and a nitrogen flow to remove water quickly. Meanwhile, four solutions were prepared: 0.1285 g NaCl in 10 ml EG (220 mmol/l), 0.0814 g  $\text{Fe}(\text{NO}_3)_3$  in 10 ml EG (33 mmol/l), 0.2625 g PVP with desired  $M_w$  in 6.25 ml EG (378 mmol/l) and 0.2625 g  $\text{AgNO}_3$  in 6.25 ml EG (247 mmol/l). After the nitrogen flow was stopped, the previous prepared solutions were added to the stirred EG in the following order with 30 sec in between each addition: 50  $\mu\text{L}$  NaCl in EG, 25  $\mu\text{L}$   $\text{Fe}(\text{NO}_3)_3$  in EG, 5.19 mL PVP in EG and 5.19 mL  $\text{AgNO}_3$  in EG. The mixture was allowed to react for a certain time without any agitation and cooled down to room temperature. Then it was equally divided into two centrifuge tubes, followed by an addition of 9 ml acetone and thoroughly vortexing. The AgNWs were collected by centrifugation at 2000 rpm for 1 h. Afterwards, the supernatant was decanted until 5 ml were left and the centrifuge tube was filled up with water. After another centrifugation step, the obtained AgNWs were washed twice with ethanol (2000 rpm, 1 h) and redispersed in EtOH.

### Electrode fabrication

Pre-cleaned and oxygen plasma treated ( $2 \times 10^{-1}$  mbar, 10 min.) BK7 glass substrates (Schott, Mainz, Germany) were used. Ethanolic dispersions of synthesized AgNWs were sonicated for 2 min and then spray-coated with a nozzle (Fisnar, Wayne (NJ), USA) onto a heated substrate (80 °C) with a spraying distance, a moving speed and a spraying pressure of the nozzle of 12 cm, 1.5 cm/s and 200 mbar, respectively.

### Characterization

High resolution transmission electron microscopy (HR-TEM) was carried out on a FEI Tecnai F30 microscope operated at an accelerating voltage of 300 kV. Scanning electron microscopy (SEM) imaging was performed on a Zeiss DSM 982 Gemini instrument operating at 10 kV.

A four-point-probe setup (Lucas Labs, USA) was used for measuring sheet resistances of obtained electrodes. Optical characterization was carried out using an UV-VIS NIR photo spectrometer with integrating sphere unit (Shimadzu, Japan). All transmission values are reported including the substrate transmission.

## Conflicts of interest

The authors declare no competing financial interest.

## Acknowledgements

This work was funded within the DFG Cluster of Excellence "Center for Advancing Electronics Dresden" (cfaed). We thank Susanne Goldberg for measuring SEM, Tobias Günther and Andreas Wendel for sample preparation, Sven Kunze and Andreas Büst for maintenance of the measurement systems, Thomas Gemming for support in HR-TEM imaging, and Donato Spoltore for discussions regarding the OSCs.

## References

- W. Gaynor, S. Hofmann, M. G. Christoforo, C. Sachse, S. Mehra, A. Salleo, M. D. McGehee, M. C. Gather, B. Lüssem, L. Müller-Meskamp, P. Peumans and K. Leo, *Adv. Mater.*, 2013, **25**, 4006–4013.
- H.-G. Cheong, R. E. Triambulo, G.-H. Lee, I.-S. Yi and J.-W. Park, *ACS Appl. Mater. Interfaces*, 2014, **6**, 7846–7855.
- S. Cho, S. Kang, A. Pandya, R. Shanker, Z. Khan, Y. Lee, J. Park, S. L. Craig and H. Ko, *ACS Nano*, 2017, **11**, 4346–4357.
- J. Lee, P. Lee, H. Lee, D. Lee, S. S. Lee and S. H. Ko, *Nanoscale*, 2012, **4**, 6408.
- Y. Park, L. Bormann, L. Müller-Meskamp, K. Vandewal and K. Leo, *Org. Electron.*, 2016, **36**, 68–72.
- F. Selzer, N. Weiß, D. Kneppel, L. Bormann, C. Sachse, N. Gaponik, A. Eychmüller, K. Leo and L. Müller-Meskamp, *Nanoscale*, 2015, **7**, 2777–2783.
- P. Zhang, I. Wyman, J. Hu, S. Lin, Z. Zhong, Y. Tu, Z. Huang and Y. Wei, *Mater. Sci. Eng. B Solid-State Mater. Adv. Technol.*, 2017, **223**, 1–23.
- T. Sanniccolo, M. Lagrange, A. Cabos, C. Celle, J. P. Simonato and D. Bellet, *Small*, 2016, **12**, 6052–6075.
- D. Langley, G. Giusti, C. Mayousse, C. Celle, D. Bellet and J.-P. Simonato, *Nanotechnology*, 2013, **24**, 452001.
- B. Wiley, Y. Sun and Y. Xia, *Acc. Chem. Res.*, 2007, **40**, 1067–76.
- V. A. Online, N. Murshid and V. Kitaev, 2014, 1247–1249.
- S. M. Bergin, Y.-H. Chen, A. R. Rathmell, P. Charbonneau, Z.-Y. Li and B. J. Wiley, *Nanoscale*, 2012, **4**, 1996–2004.
- M. Tsuji, Y. Nishizawa, K. Matsumoto, M. Kubokawa, N. Miyamae and T. Tsuji, *Mater. Lett.*, 2006, **60**, 834–838.
- X. Zeng, B. Zhou, Y. Gao, C. Wang, S. Li, C. Y. Yeung and W.



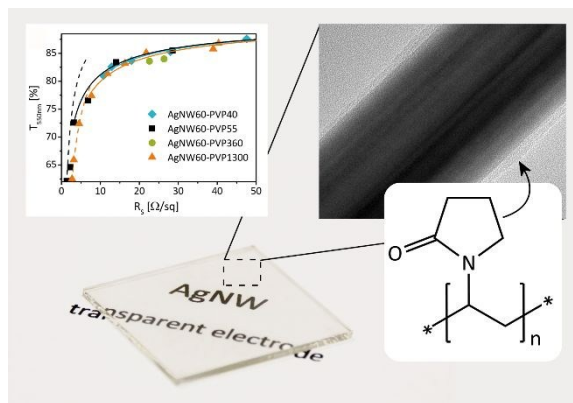
- Wen, *Nanotechnology*, 2014, **25**, 495601.
- 15 J.-J. Zhu, C.-X. Kan, J.-G. Wan, M. Han and G.-H. Wang, *J. Nanomater.*, 2011, **2011**, 1–7.
- 16 B. Li, S. Ye, I. E. Stewart, S. Alvarez and B. J. Wiley, *Nano Lett.*, 2015, **15**, 6722–6726.
- 17 Q. Xue, W. Yao, J. Liu, Q. Tian, L. Liu, M. Li, Q. Lu, R. Peng and W. Wu, *Nanoscale Res. Lett.*, 2017, **12**, 480.
- 18 N. de Guzman and M. D. L. Balela, *J. Nanomater.*, 2017, **2017**, 1–14.
- 19 Y.-J. Song, M. Wang, X.-Y. Zhang, J.-Y. Wu and T. Zhang, *Nanoscale Res. Lett.*, 2014, **9**, 17.
- 20 Y. Ran, W. He, K. Wang, S. Ji and C. Ye, *Chem. Commun.*, 2014, **50**, 14877–14880.
- 21 Y. Jia, C. Chen, D. Jia, S. Li, S. Ji and C. Ye, *ACS Appl. Mater. Interfaces*, 2016, acsami.6b00500.
- 22 N. Weiß, L. Müller-Meskamp, F. Selzer, L. Bormann, A. Eychmüller, K. Leo and N. Gaponik, *RSC Adv.*, 2015, **5**, 19659–19665.
- 23 F. Selzer, N. Weiß, L. Bormann, C. Sachse, N. Gaponik, L. Müller-Meskamp, A. Eychmüller and K. Leo, *Org. Electron.*, 2014, **15**, 3818–3824.
- 24 T. Tokuno, M. Nogi, M. Karakawa, J. Jiu, T. T. Nge, Y. Aso and K. Suganuma, *Nano Res.*, 2011, **4**, 1215–1222.
- 25 J. H. Seo, I. Hwang, H.-D. Um, S. Lee, K. Lee, J. Park, H. Shin, T.-H. Kwon, S. J. Kang and K. Seo, *Adv. Mater.*, 2017, **29**, 1701479.
- 26 Y. Ge, X. Duan, M. Zhang, L. Mei, J. Hu, W. Hu and X. Duan, *J. Am. Chem. Soc.*, 2017, jacs.7b07851.
- 27 F. Xu, W. Xu, B. Mao, W. Shen, Y. Yu, R. Tan and W. Song, *J. Colloid Interface Sci.*, 2018, **512**, 208–218.
- 28 B. Wiley, Y. Sun and Y. Xia, *Langmuir*, 2005, **21**, 8077–8080.
- 29 A. Kyrychenko, O. M. Korsun, I. I. Gubin, S. M. Kovalenko and O. N. Kalugin, *J. Phys. Chem. C*, 2015, **119**, 7888–7899.
- 30 M. del P. Buera, G. Levi and M. Karel, *Biotechnol. Prog.*, 1992, **8**, 144–148.
- 31 B. C. Hancock and G. Zografi, *Pharm. Res.*, 1994, **11**, 471–477.
- 32 R. Nair, N. Nyamweya, S. Gönen, L. J. Martínez-Miranda and S. W. Hoag, *Int. J. Pharm.*, 2001, **225**, 83–96.
- 33 S. Vijaykumar, S. Prasannkumar, B. S. Sherigara, N. B. Shelke, T. M. Aminabhavi and B. S. R. Reddy, *Macromol. Res.*, 2009, **17**, 1003–1009.
- 34 M. Lagrange, D. P. Langley, G. Giusti, C. Jiménez, Y. Bréchet and D. Bellet, *Nanoscale*, 2015, **7**, 17410–23.
- 35 D. P. Langley, M. Lagrange, G. Giusti, C. Jiménez, Y. Bréchet, N. D. Nguyen and D. Bellet, *Nanoscale*, 2014, **6**, 13535–13543.
- 36 M. E. Toimil Molares, A. G. Balogh, T. W. Cornelius, R. Neumann and C. Trautmann, *Appl. Phys. Lett.*, 2004, **85**, 5337–5339.
- 37 F. Ruffino and M. G. Grimaldi, *Phys. status solidi*, 2015, **212**, 1662–1684.
- 38 T. Müller, K.-H. Heinig and B. Schmidt, *Mater. Sci. Eng. C*, 2002, **19**, 209–213.
- 39 S. De, P. J. King, P. E. Lyons, U. Khan and J. N. Coleman, *ACS Nano*, 2010, **4**, 7064–7072.
- 40 H. Wang, K. Li, Y. Tao, J. Li, Y. Li, L.-L. Gao, G.-Y. Jin and Y. Duan, *Nanoscale Res. Lett.*, 2017, **12**, 77.
- W. Gaynor, G. F. Burkhard, M. D. McGehee and P. Peumans, *Adv. Mater.*, 2011, **23**, 2905–10.
- R. Meerheim, C. Körner and K. Leo, *Appl. Phys. Lett.*, 2014, **105**, 063306.
- L. Bormann, F. Nehm, L. Sonntag, F.-Y. Chen, F. Selzer, L. Mueller-Meskamp, A. Eychmüller and K. Leo, *ACS Appl. Mater. Interfaces*, 2016, **8**, 14709–14716.

View Article Online

DOI: 10.1039/C9PC00680J

Open Access Article. Published on 13 March 2019. Downloaded on 3/14/2019 11:41:56 AM.  
This article is licensed under a Creative Commons Attribution-NonCommercial 3.0 Unported Licence.





Improving the performance of Ag nanowire electrodes by adjusting reaction conditions and the molecular weight of PVP.

